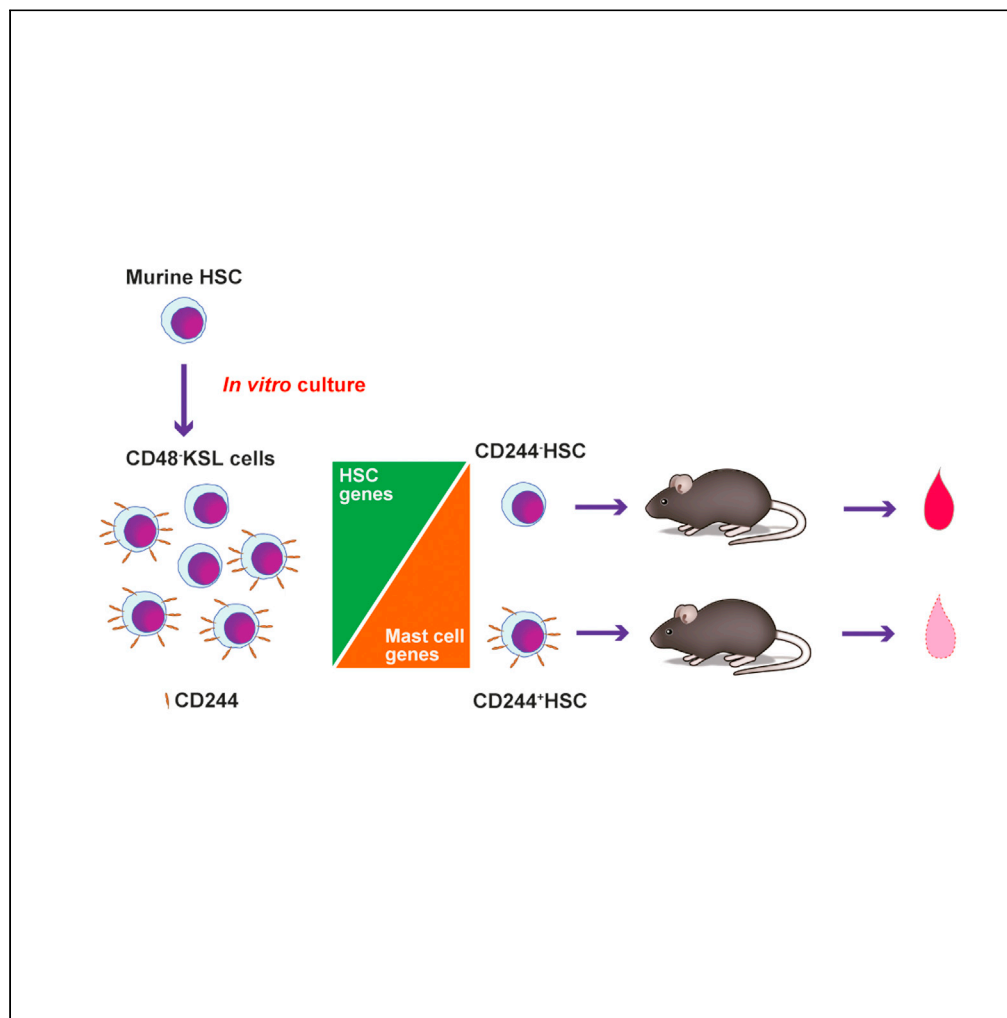


Article

CD244 expression represents functional decline of murine hematopoietic stem cells after *in vitro* culture



Shuheikoide,
Valgardur
Sigurdsson, Visnja
Radulovic, ...,
Shamit Soneji,
Atsushi Iwama,
Kenichi Miharada

kenmiharada@kumamoto-u.
ac.jp

Highlights

Murine HSCs up-regulate
mast cell-related genes
including *Cd244* during *in
vitro* culture

Long-term HSCs after *in
vitro* culture are enriched
in CD244⁻CD48⁻KSL
population

Induction of unfolded
protein response is
involved in the increase of
CD244⁺HSC

Koide et al., iScience 25,
103603
January 21, 2022 © 2021 The
Author(s).
[https://doi.org/10.1016/
j.isci.2021.103603](https://doi.org/10.1016/j.isci.2021.103603)



Article

CD244 expression represents functional decline of murine hematopoietic stem cells after *in vitro* culture

Shuheikoide,^{1,2,5} Valgardur Sigurdsson,^{1,5} Visnja Radulovic,¹ Kiyoka Saito,^{1,3} Zhiqian Zheng,² Stefan Lang,⁴ Shamit Soneji,⁴ Atsushi Iwama,² and Kenichi Miharada^{1,3,6,*}

SUMMARY

Isolation of long-term hematopoietic stem cell (HSC) is possible by utilizing flow cytometry with multiple cell surface markers. However, those cell surface phenotypes do not represent functional HSCs after *in vitro* culture. Here we show that cultured HSCs express mast cell-related genes including *Cd244*. After *in vitro* culture, phenotypic HSCs were divided into CD244⁻ and CD244⁺ subpopulations, and only CD244⁻ cells that have low mast cell gene expression and maintain HSC-related genes sustain reconstitution potential. The result was same when HSCs were cultured in an efficient expansion medium containing polyvinyl alcohol. Chemically induced endoplasmic reticulum (ER) stress signal increased the CD244⁺ subpopulation, whereas ER stress suppression using a molecular chaperone, TUDCA, decreased CD244⁺ population, which was correlated to improved reconstitution output. These data suggest CD244 is a potent marker to exclude non-functional HSCs after *in vitro* culture thereby useful to elucidate mechanism of functional decline of HSCs during *ex vivo* treatment.

INTRODUCTION

Hematopoietic stem cells (HSCs) replenish the entire blood system when needed, and transplantation of HSCs remains as one of the most effective treatments for patients with genetic diseases and hematopoietic malignancies (Seita and Weissman, 2010). Identification of multiple cell surface markers, e.g., c-Kit, Sca-1, CD34, SLAM family members, EPCR, CD45RA, CD49f, and CD90 (Balazs et al., 2006; Kiel et al., 2005; Notta et al., 2011; Oguro et al., 2013; Osawa et al., 1996), and utilization of unique cellular properties, e.g., dye-efflux and high aldehyde dehydrogenase 1-A1 activity (Goodell et al., 1996; Storms et al., 1999), have enabled prospective isolation of HSCs from bone marrow (BM) and umbilical cord blood. To this day, long-term reconstitution into recipient mice remains as the only reliable test of HSC functionality. In steady state (dormant) conditions, HSCs can be successfully enriched; however, surface marker phenotypes change and become distorted upon multitude of hematopoietic stress, e.g., inflammation and *ex vivo* culture (Zhang and Lodish, 2005). Functionality of HSCs is especially difficult to predict after *in vitro* cell culture, solely based on phenotype, even though we rely heavily on it to study normal and malignant HSC biology. One of the few markers that have been proposed to predict reconstitution potential after *in vitro* culture is CD48, as functional HSCs are enriched in the CD48⁻ fraction within c-kit⁺Sca-1⁺Lineage⁻ (KSL) cell population after culture (Noda et al., 2008). Yet, CD48 negativity cannot always represent HSC functionality. For instance, we and others have previously demonstrated that HSCs in culture are vulnerable to endoplasmic reticulum (ER) stress responses fueled by accumulation of unfolded/misfolded proteins (Miharada et al., 2014; van Galen et al., 2014; Walter and Ron, 2011). In our previous work we could ameliorate ER stress pathways using bile acids (BAs) and significantly enhance reconstitution potential of HSCs after *in vitro* culture (Miharada et al., 2014; Sigurdsson et al., 2016). However, a standard HSC staining including CD48 was not able to point out noticeable differences between samples cultured with or without BA, indicating increased functionality (Miharada et al., 2014). The discovery of additional cell surface markers that correlate with reconstitution capacity after *in vitro* culture would be highly beneficial and reduce dependency on the transplantation assay in HSC biology.

In this study our aim was to discover key signatures and cell surface markers representing the functional decline of HSCs during *ex vivo* culture. We performed gene expression profiling to compare fresh and

¹Division of Molecular Medicine and Gene Therapy, Lund Stem Cell Center, Lund University, 221 84 Lund, Sweden

²Division of Stem Cell and Molecular Medicine, Center for Stem Cell Biology and Regenerative Medicine, The Institute of Medical Science, The University of Tokyo, 108-0071 Tokyo, Japan

³International Research Center for Medical Sciences, Kumamoto University, 860-0811 Kumamoto, Japan

⁴StemTherapy Bioinformatics Core Facility, Lund Stem Cell Center, Lund University, 221 84 Lund, Sweden

⁵These authors contributed equally

⁶Lead contact

*Correspondence: kenmiharada@kumamoto-u.ac.jp

<https://doi.org/10.1016/j.isci.2021.103603>



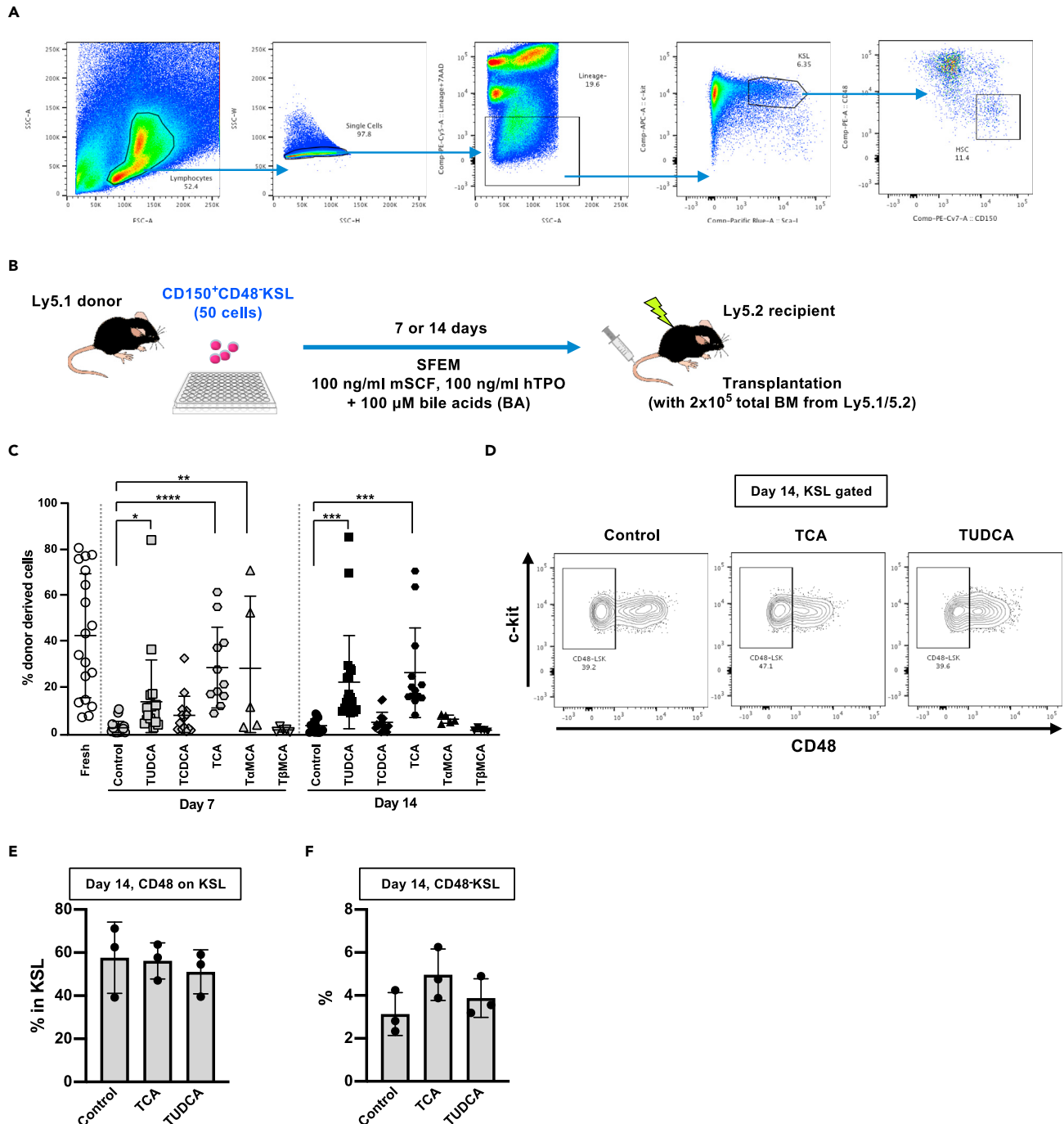


Figure 1. Transplantation of HSCs cultured with various bile acids

(A) The gating strategy for isolating CD150⁺CD48⁻KSL cells from murine bone marrow.

(B) Experimental design of the competitive reconstitution assay. Fifty (50) CD150⁺CD48⁻KSL cells were isolated from BM of Ly5.1 mice (donor, two mice per experiment were used) and cultured in Stemspan SFEM medium supplemented with 100 ng/mL mSCF and 100 ng/mL hTPO with or without 100 μ M of different types of bile acids (BA) for 7 or 14 days. Cells were then transplanted into lethally irradiated Ly5.2 mice (recipient, 5–18 mice) along with 2×10^5 total BM cells derived from Ly5.1/5.2 (F1) mice (competitor). Donor contribution (chimerism) was monitored by analyzing peripheral blood (PB) every month.

Figure 1. Continued

(C) Peripheral blood analysis of the transplanted mice. Chimerism in PB at 16 weeks of transplanted mice are shown. Mean \pm SD from three independent experiments (n = 5–18) are displayed. Significance was calculated using one-way ANOVA within the same culture days. * $p < 0.05$, ** $p < 0.01$, *** $p < 0.001$, **** $p < 0.0001$.

(D–F) Cell surface expression of CD48 on KSL fraction of HSCs cultured with or without BA. Representative FACS plots (C) and summary of the flow cytometry analyses (D and E) are shown. Mean \pm SD (n = 3) are displayed.

cultured HSCs and discovered up-regulation of genes that are highly expressed in mast cells. In addition, we identified *Cd244* as one of the top up-regulated genes. After *in vitro* culture, HSC population represented by CD48[−]KSL was subdivided into CD244⁺ and CD244[−] populations. CD244[−]CD48[−]KSL expressed high levels of HSC-related genes, whereas CD244⁺CD48[−]KSL expressed mast cell-related genes, and only CD244[−]CD48[−]KSL cells exhibited long-term reconstitution potential. ER stress induction is correlated to CD244 expression, as treatment with an ER stress inducer, tunicamycin, reduced the ratio of CD244[−]CD48[−]KSL cells, whereas addition of the BA, TUDCA, increased the ratio of CD244[−] HSCs. Furthermore, this was also the case when HSCs were cultured in the efficient expansion medium containing polyvinyl alcohol (PVA) (Wilkinson et al., 2019).

Our data show that CD244 is a potent marker to represent functionally impaired HSCs enabling prospective evaluation of HSC after extensive *in vitro* culture.

RESULTS**CD48 is unable to distinguish functional HSCs after *in vitro* culture**

We have previously reported that two specific types of BAs, TUDCA and taurocholic acid (TCA), can maintain functionality of HSCs *in vitro* (Miharada et al., 2014; Sigurdsson et al., 2016); however, no clear difference was observed in the frequency of CD48[−]KSL cells after *in vitro* culture of fetal liver HSCs (Sigurdsson et al., 2016). To reproduce the result using adult HSCs from murine BM, CD150⁺CD48[−]KSL cells were cultured with different BA, analyzed, and transplanted into lethally irradiated mice (Figures 1A and 1B). Peripheral blood (PB) analyses showed that long-term engraftment of HSCs cultured with TUDCA and TCA was significantly higher than under other conditions (Figure 1C). Flow cytometry analyses of cultured HSCs using KSL and CD48 staining did not show significant differences between TUDCA/TCA and control condition, despite showing improvement in transplantation chimerism (Figures 1D–1F). These results suggest that CD48 negativity is not sufficient to detect HSC functionality after *in vitro* culture.

Induction of mast cell-related genes in HSCs after *in vitro* culture

To discover transcriptional changes occurring during the *in vitro*-cultured HSCs and to identify additional markers that represent functionality/impairment of HSCs after *in vitro* culture, we performed a gene expression profiling of freshly isolated HSCs compared with *in vitro*-cultured HSCs. CD48[−]KSL cells were freshly isolated from 10-week-old mice (YF) and then cultured in serum-free medium supplemented with 100 ng/mL of murine stem cell factor (mSCF) and human thrombopoietin (hTPO) for 14 days, and then CD48[−]KSL cells were re-isolated (YC) (Figure 2A). Comparison of transcriptional profiles of these samples revealed significant changes of gene expression patterns (Figure 2B). Genes down-regulated upon *in vitro* culture mainly included genes that are known for their functions in HSC regulations or as markers of HSCs, e.g., *Klf4*, *Procr*, *Fgd5*, *Hlf*, *Nr4a1*, and *Nr4a2* (Balazs et al., 2006; Calvanese et al., 2019; Freire and Conneely, 2018; Gazit et al., 2014; Komorowska et al., 2017; Park et al., 2019). This might suggest that the CD48[−]KSL population contains only a small fraction of functional HSCs and/or cells with profoundly reduced HSC function after *in vitro* culture. In contrast, up-regulated genes included genes that are normally highly expressed in mast cells, such as *Mcpt1/2/4/8*, *Cpa3*, *Cma1*, *Ccl2*, and *Gzmb* (Dwyer et al., 2016) (Figure 2C). Using gene set enrichment analysis (GSEA) (Subramanian et al., 2005) we could identify a variety of gene signatures that changed between samples (Table S1) including loss of a long-term HSC signature and induction of the mast cell signature (Figure 2D). In addition, signature of unfolded protein response (UPR) induction was found in the cultured HSCs (Figure 2D), in line with our previous study (Miharada et al., 2014).

Mast cells are immune cells playing major roles in pathogen surveillance as well as promoting host defense through cellular communications with other immune cell types (Abraham and St John, 2010). Mast cells are characterized by existence of histamine-rich granules that are released upon various stimulations, particularly immunoglobulin E (IgE) binding to their cell surface FC receptor, which is a key reaction during allergic responses (Galli and Tsai, 2012). Expression of multiple mast cell-related genes including mature mast cell

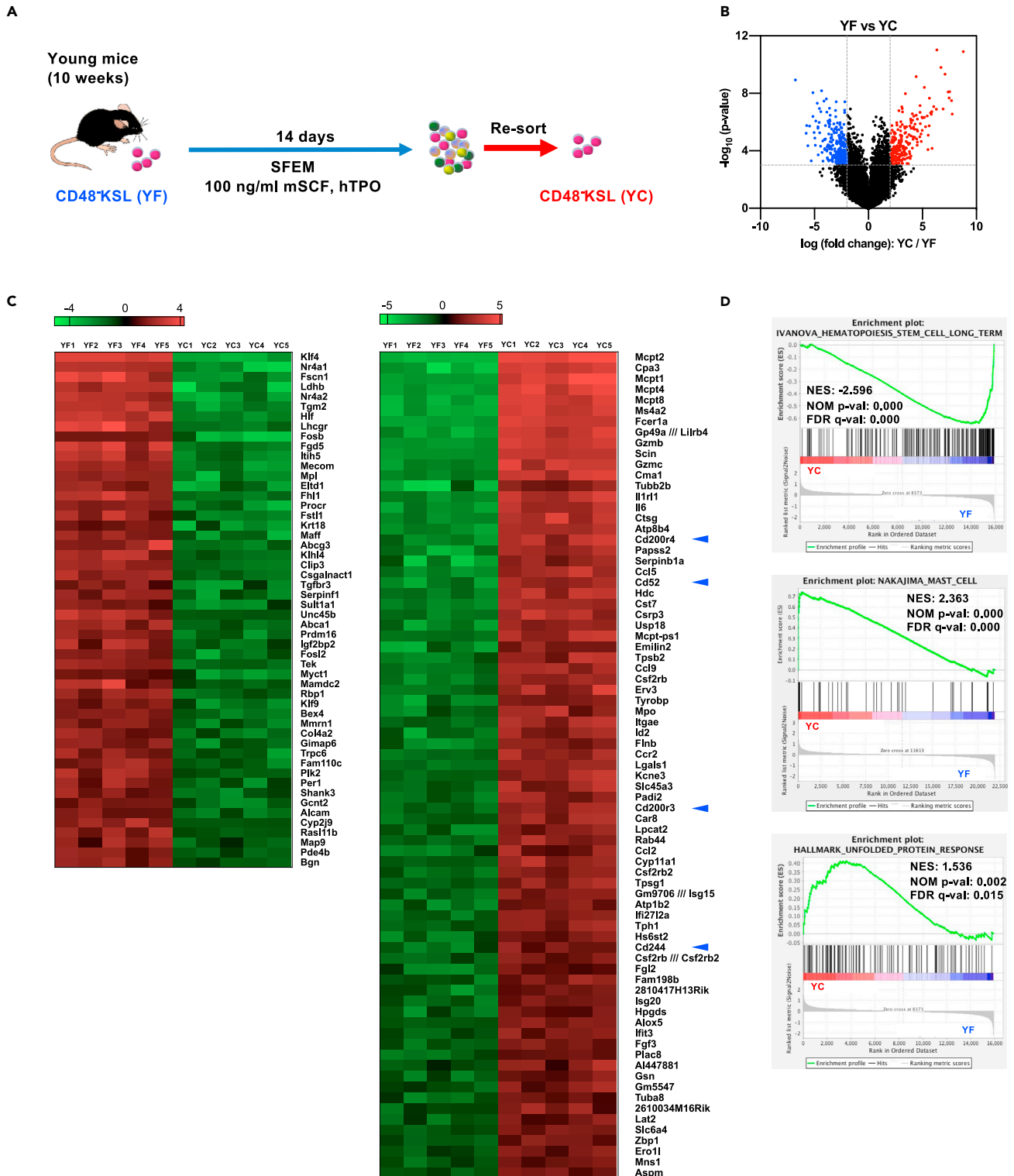


Figure 2. Gene expression changes in CD48⁺KSL cells upon *in vitro* culture and aging

(A) Experimental design of the gene expression analysis. Five hundred CD48⁺KSL cells were sorted from BM of young (10 weeks old, YF) mice. Cells were also cultured in Stemspan SFEM medium supplemented with 100 ng/mL mSCF and 100 ng/mL hTPO for 14 days, and CD48⁺KSL cells were re-sorted.

(B) Volcano plot showing differentially expressed genes between YF and YC. Significant difference was defined as $p < 0.001$ and \log_2 fold change < -2 (blue) or > 2 (red).

Figure 2. Continued

(C) Heatmaps showing a list of differentially expressed genes. Significant difference was defined as $p < 0.0001$ and \log_2 fold change < -3 or > 3 . Blue arrowheads indicate CD markers.

(D) Gene set enrichment analysis (GSEA) of the microarray data comparing YF and YC. NES, normalized enrichment score; NOM p-val, nominal p value; FDR q-val, false discovery rate q-value. See also [Table S1](#).

genes such as *Fcer1a*, which codes *FcεRIα*, were observed in the YC cells. However, flow cytometry analysis was not able to detect *FcεRI* protein on the cell surface and morphological analyses of re-isolated YC cells did not observe the typical granule-rich morphology (data not shown), suggesting that YC cells were not fully differentiated toward mast cells. Mast cells are known to share crucial genes with basophils (Dwyer et al., 2016), but GSEA did not observe enrichment of a basophil signature in both cultured CD48⁻KSL cells and CD244⁺CD48⁻KSL cells (data not shown). SCF is a strong inducer of mast cell differentiation, whereas TPO signaling is considered to inhibit mast cell differentiation (Martelli et al., 2008). Both SCF and TPO are used as standard cytokines in mouse and human HSC culture. However, our gene expression analysis showed that expression levels of *Mpl*, TPO receptor, were significantly down-regulated (Figure 2C), presumably failing to suppress induction of mast cell genes during the *in vitro* culture.

Aging is also known as a trigger of functional decline of HSC (Sudo et al., 2000). Therefore, we also analyzed if aging stress also induces mast cell signature. Gene expression profiles of HSCs isolated from young mice (YF) and from aged (18 months) mice (AF) were compared (Figure S1A). GSEA revealed that the mast cell signature was rather enriched in YF (Figure S1B). This finding indicates that induction of UPR genes and the mast cell signature might be specific for *ex vivo* culture conditions.

CD244 can functionally subdivide the CD48⁻KSL population after *in vitro* culture

We identified that the cell surface marker *Cd244* was one of the significantly up-regulated genes in the *in vitro*-cultured CD48⁻KSL cells (Figure 2C). *Cd244* is a member of the SLAM family of genes and is expressed in various immune cells including NK cells, $\gamma\delta$ T cells, CD8⁺ $\alpha\beta$ T cells, monocytes, basophils, eosinophils, dendritic cells, and mast cells (McArdel et al., 2016). The CD244 molecule plays roles in immune responses partially through its binding to CD48 (Agresta et al., 2018; Elishmereni et al., 2014; Waggoner and Kumar, 2012). CD244 has been reported as a negative marker for HSC isolation but is currently considered to be redundant with other SLAM markers when purifying fresh HSCs from steady-state mice (Kiel et al., 2005; Oguro et al., 2013). Freshly isolated CD150⁺CD48⁻LSK cells were mostly negative for CD244, whereas after *in vitro* culture for 14 days CD48⁻KSL cells were subdivided into CD244⁺ and CD244⁻ populations and a vast majority of CD48⁺ cells were CD244⁺ (Figures 3A and 3B). The expression pattern of two frequently used HSC markers, CD34 and CD150 (Kiel et al., 2005; Osawa et al., 1996), was abnormal compared with freshly isolated cells (Figure S2A). We also checked the expression of EPCR (Procr, CD201) on the cultured cells, since EPCR is known as a potent marker of human HSCs both before and after *in vitro* culture and to enrich for functional murine HSC after 5-FU treatment (Fares et al., 2017; Umemoto et al., 2018). Flow cytometry analyses of cultured HSCs showed that a vast majority of CD244⁻KSL cells were positive for EPCR while EPCR⁺KSL cells contained both CD244⁺ and CD244⁻ fractions (Figure S2A). To compare the proliferative status of CD244⁻CD48⁻KSL cells (CD244⁻HSCs) and CD244⁺CD48⁻KSL cells (CD244⁺HSCs), cell cycle profiles of these subpopulations were analyzed using Ki-67 staining after 7 days' culture. CD244⁻HSCs contained the highest proportion of Ki-67-positive cells, indicating least cycling of this population (Figures S2B and S2C). In addition, we measured protein synthesis rates in different subpopulations using L-homopropargylglycine (L-HPG) incorporation into newly synthesized proteins. The results indicate that CD244⁻CD48⁻KSL cells have the lowest protein synthesis levels among the different subgroups. However, between CD244⁻HSCs and CD244⁺HSCs there was not a significant difference (Figures S2D and S2E). To further characterize these subpopulations, CD244⁻HSCs and CD244⁺CD244⁺HSCs were isolated from 7-day cultured HSC samples (Figure 3C) and expression levels of representative genes in HSCs or mast cell regulation were analyzed using quantitative RT-PCR. Significantly higher expression levels of HSC-related genes (*Fgd5*, *Hlf*, *Fhl1* and *Mpl*) were observed in CD244⁻HSCs, whereas higher expression of mast cell-related genes (*Cpa3*, *Gzmb*, and *Mcpt8*) was detected in CD244⁺HSCs (Figure 3D). However, morphologies of these two types of HSCs are similar (Figure S2F).

To compare long-term reconstitution potential of these two populations, CD244⁻ and CD244⁺ HSCs were separately isolated from 7-day cultured HSC samples and transplanted into lethally irradiated mice. Monthly PB analysis showed that CD244⁻HSCs showed long-term reconstitution of the hematopoietic system of transplanted mice while engraftment levels of CD244⁺HSCs was low (Figure 3E). Both CD244⁻ and

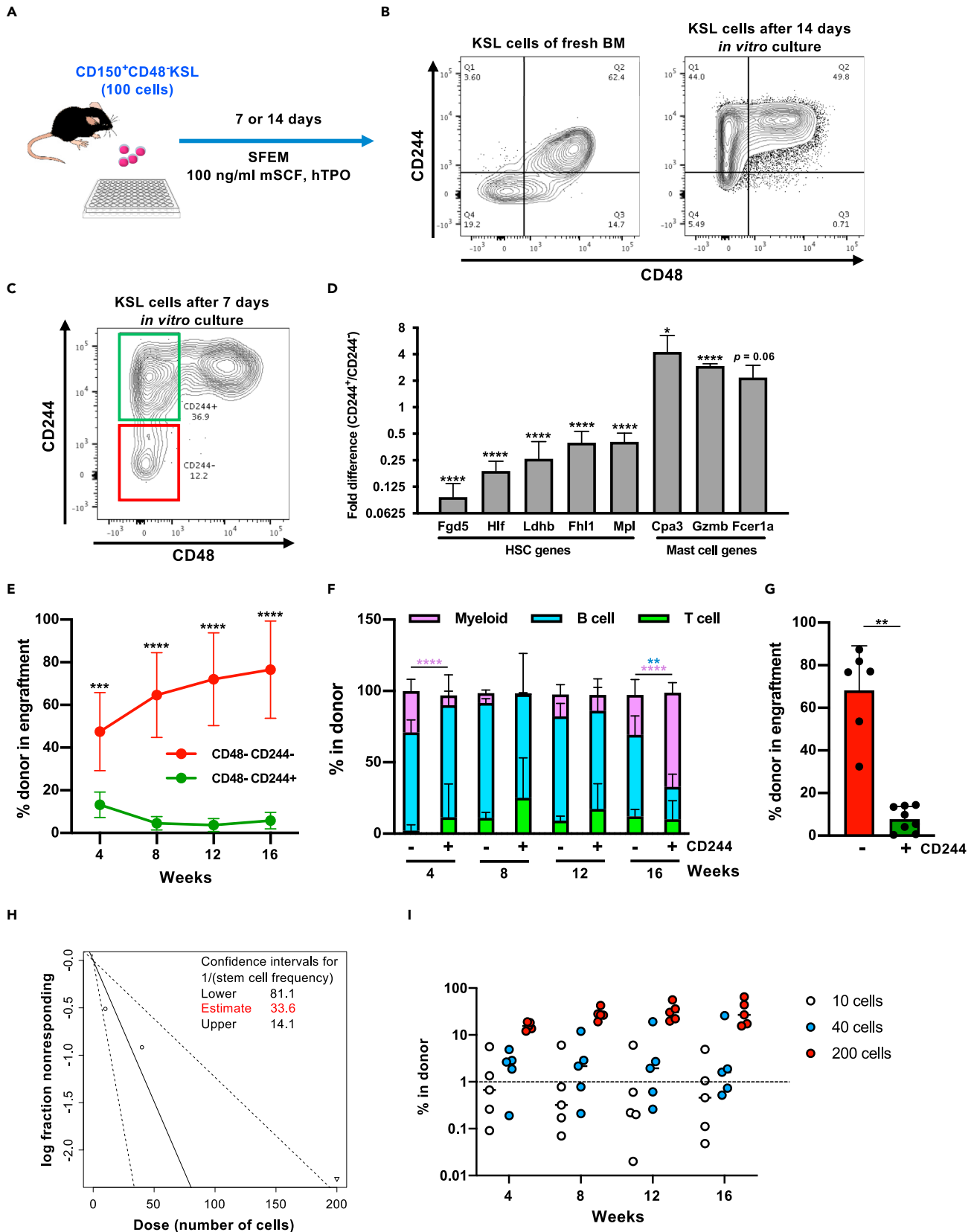


Figure 3. CD244 expression divides CD48⁻ KSL cells into functionally distinct subpopulations after *in vitro* culture

(A) Experimental design of the *in vitro* culture experiment. One hundred CD48⁻KSL cells were sorted from BM of young mice and cultured in Stemspan SFEM medium supplemented with 100 ng/mL mSCF and 100 ng/mL hTPO for 7 days.

(B) Expression patterns of CD244 and CD48 on the cell surface of fresh and 14 days cultured KSL cells. Representative FACS plots on KSL population are shown.

(C and D) qRT-PCR analysis for HSC-related genes and mast cell-related genes in CD244⁺CD48⁻KSL cells compared with the CD244⁺CD48⁻KSL counterpart. Representative FACS plot and gating of CD244⁺CD48⁻KSL cells (green) and CD244⁻CD48⁻KSL cells (red) on 7 days cultured KSL cells are shown in (C). Relative expression levels of genes in CD244⁺CD48⁻KSL cells to CD244⁻CD48⁻KSL are shown in (D).

(E) Competitive reconstitution assay. After 7 days' culture, two subpopulations were sorted and 1,000 of CD244⁻ or 1,500 of CD244⁺CD48⁻KSL cells were separately transplanted into lethally irradiated recipient mice (seven mice) with 2×10^5 total BM cells (competitor). Chimerism was monitored by analyzing PB every month. Significance was calculated using Student's *t* test at each time point. Mean \pm SD from two independent experiments (*n* = 7) are displayed. *****p* < 0.0001.

(F) Lineage balance of donor-derived cells in the PB of recipient mice. Mean \pm SD from two independent experiments (*n* = 6) are displayed. ***p* < 0.01, *****p* < 0.0001. Each color represents different lineages.

(G) Analysis of BM from engrafted mice after 16 weeks. Chimerism in each cell fraction is shown. Significance was calculated using Student's *t* test. Mean \pm SD from two independent experiments (*n* = 6) are displayed. ***p* < 0.01.

(H and I) Limiting dilution assay for CD244⁻CD48⁻KSL cells. CD244⁻CD48⁻KSL cells were re-sorted after 7 days' *in vitro* culture and 200, 40, or 10 cells were transplanted to recipient mice in a competitive manner. Chimerism above 1% was judged as successful engraftment. The frequency of functional HSC was calculated using ELDA (<http://bioinf.wehi.edu.au/software/elda/>). Chimerism of individual mice is shown in (I).

CD244⁺HSCs reconstituted Myeloid, B, and T cells with a modest difference; however, the PB profile of CD244⁺HSC-engrafted mice was not accurate because of their low engraftment levels (Figure 3F). Analyses of BM of the transplanted mice revealed that the reconstitution level of CD244⁻HSCs was significantly higher than that of CD244⁺HSCs (Figure 3G). In order to estimate the frequency of functional HSC within the CD244⁻CD48⁻KSL fraction, limiting dilution assay was performed. After 7 days of culture, CD244⁻CD48⁻KSL cells were re-sorted and 10, 40, and 200 cells were transplanted into lethally irradiated recipient mice in a competitive manner. From this experiment we estimate the HSC frequency in the CD244⁻CD48⁻KSL fraction to be 1/33.6 cells (Figures 3H and 3I).

In summary, our experiments indicate that the CD244⁻CD48⁻KSL fraction in culture is distinct from CD244⁺ cells and highly enriched for functional HSCs.

ER stress induction and cytokine signals affect CD244 expression

We and others have previously demonstrated that induction of UPR and ER stress signals impair the potential of mouse and human HSCs (Miharada et al., 2014; van Galen et al., 2014) during *in vitro* culture. These results were also confirmed with our gene expression analysis in this study (Figure 2D). We therefore asked if ER stress induction would lead to the elevation of CD244 expression. Addition of a chemical ER stress inducer, tunicamycin, increased the ratio of CD244⁺HSCs within CD48⁻KSL cells (Figures 4A and 4B). Conversely, addition of TUDCA, a BA known to suppress ER stress (Miharada et al., 2014; Özcan et al., 2006; Sigurdsson et al., 2020), resulted in increased frequency of CD244⁻HSCs (Figures 4A and 4B). Of note, the frequency of KSL cells did not significantly differ in both cases and CD48 negativity was marginally affected while the frequency of CD244⁻CD48⁻ population in KSL was significantly changed (Figure 4B).

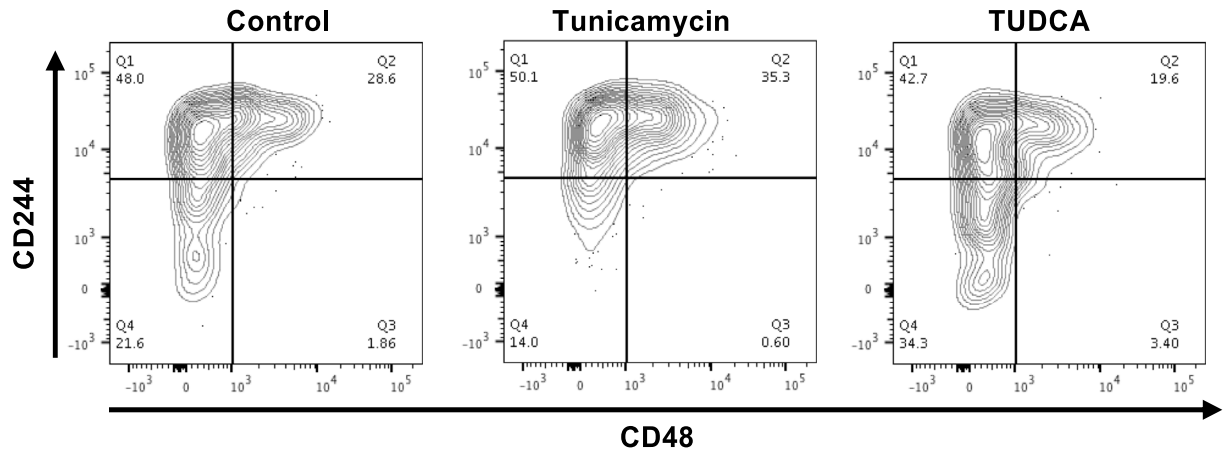
Since TPO signaling is known to inhibit mast cell differentiation (Martelli et al., 2008), we next analyzed the influence of cytokine concentration during the *in vitro* culture on the frequency of the CD244⁻CD48⁻KSL population. High TPO and low SCF concentrations have recently been reported as the optimal culture condition for HSCs (Kobayashi et al., 2019; Wilkinson et al., 2019). In contrast, our results showed that a combination of high concentration (100 ng/mL) of both SCF and TPO maintained the highest CD244⁻CD48⁻KSL population in culture. Although lower concentrations of SCF and TPO both resulted in lower frequency of the CD244⁻CD48⁻KSL fraction, there was a tendency that a lower concentration of TPO reduced the CD244⁻CD48⁻KSL fraction more than the same SCF concentration (Figures 4C and S3).

These findings indicate that *in vitro* culture-induced ER stress and cytokine signals could be one of the critical causes of functional impairment of HSCs in cell culture that can be measured by CD244 elevation.

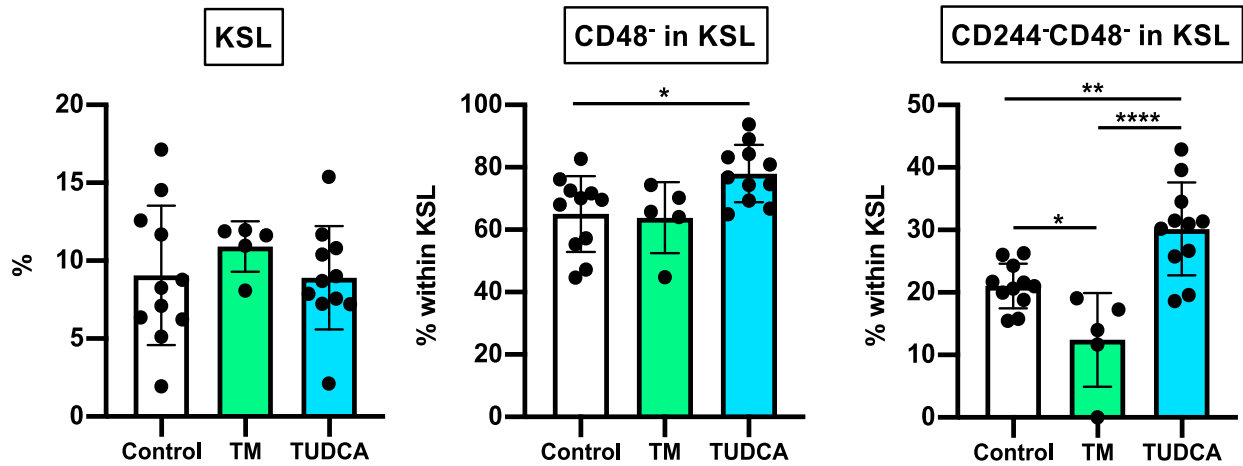
Gene expression profiling of CD244⁻ and CD244⁺ HSCs

To explore the key molecular changes that impair HSC functionality, we compared gene expression profiles between fresh HSCs and CD244⁺/CD244⁻HSCs after 7 days' culture in the conventional culture condition.

A



B



C

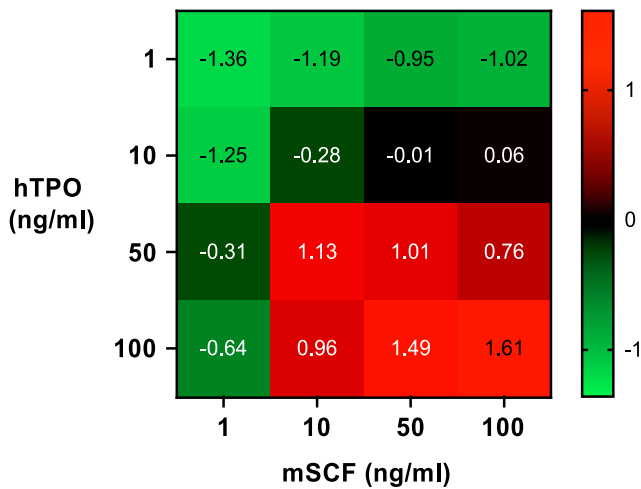


Figure 4. ER stress induction and cytokine signals affect CD244 expression

(A) Expression patterns of CD244 and CD48 on KSL cells after *in vitro* culture in Stemspan SFEM medium supplemented with 100 ng/mL mSCF and 100 ng/mL hTPO for 7 days, and with or without 0.5 μ g/mL Tunicamycin or 100 μ M TUDCA. Representative FACS plots are shown.

(B) Summary of the flow cytometry analyses. Frequencies of KSL cells, CD48⁺ fraction in KSL population, and CD244⁺CD48⁺ fraction in KSL population are shown. Mean \pm SD from two independent experiments (n = 5–11) are displayed. Significance was calculated using one-way ANOVA within each population. **p* < 0.05, ***p* < 0.01, *****p* < 0.0001.

(C) A heatmap showing frequencies of CD244⁺CD48⁺KSL cells after 7 days' culture with various SCF/TPO concentrations. Mean values of Z score (n = 3) in each fraction are displayed.

CD244⁺CD48⁺KSL cells were freshly isolated from young (8 weeks old) mice (N) and cultured for 7 days, and then CD244⁺CD48⁺KSL cells (CN) or CD244⁺CD48⁺KSL cells (CP) were re-isolated (Figure 5A). Gene expression analysis revealed that there were more differentially expressed genes between N and CN cells than between CN and CP cells, although critical functional difference was seen between CN and CP (Figure 5B). Among significantly differentially expressed genes between three types of cells, multiple expression patterns were detected; in both up- and down-regulated genes, some of the genes showed significant changes between N and CN that were at the same degree in CP cells, which were presumably more directly affected by *in vitro* culture. This group contained *Nr4a1*, *Fosb*, *Klf4*, *Mllt3*, *Gata2* (down-regulated) and *Gm40022*, *Bcat1*, *Atf5* (up-regulated) (Figure 5C). Other than these, a part of genes exhibited gradual changes in expression levels, meaning that the expression levels of those genes are more linearly correlated to the reconstitution potential of the cells. This group contained *ApoE*, *Vwf*, *Hlf*, *Procr* (down-regulated) and *Cd244*, *Ccl5*, *Nrp1*, *Cd34* (up-regulated) (Figure 5C). Similarly, GSEA on both N versus CN and CN versus CP observed significant enrichment of gene signatures in various fashions. For instance, tumor necrosis factor alpha (TNF α) signaling, epidermal growth factor (EGF) signaling, and hypoxic response signatures, which have been implicated in HSC function (Doan et al., 2013; Miharada et al., 2011; Suda et al., 2011; Yamashita and Passegué, 2019), were gradually lost in accordance with loss of reconstitution capacity (N > CN > CP), whereas cell cycle-related hallmarks, chromosome segregation, and UPR signatures were gradually induced (N < CN < CP) (Figure 5D and Table S2). In contrast, signature of transforming growth factor β (TGF β) signaling (Yamazaki et al., 2009) was uniquely enriched in N (N > CN = CP) and interferon alpha (IFN α) signaling pathway was induced in CN (N < CN = CP), suggesting that these pathways might more directly reflect environmental changes upon *in vitro* culture (Figure 5D and Table S2). Thus, including CD244 as a marker enables one to dissect cellular and molecular changes during the transformation of HSCs upon *in vitro* culture.

CD244 enriches functional HSCs after *in vitro* culture with PVA

High-efficiency *in vitro* expansion of phenotypic HSCs has been described using a culture medium containing polyvinyl alcohol (PVA) and a low concentration of SCF (Wilkinson et al., 2019). We used the CD244 marker to ask if there is functional heterogeneity in expanded HSCs after culture in PVA medium. Purified CD150⁺CD48⁺KSL cells were cultured for 7 days in PVA medium supplemented with 10 ng/mL of mSCF and 100 ng/mL of mTPO according to the original report (Figure 6A). Unlike the conventional culture condition, CD48⁺KSL population contained CD244⁺ and CD244⁺ fractions, whereas all CD244⁺KSL cells were CD48⁺ (Figure 6B). A small fraction of CD244⁺CD48⁺KSL cells (<10%) was identified in the PVA culture, and these cells were also positive for EPCR (Figure S4). Alternative analysis of the PVA data showed that CD244⁺CD48⁺KSL cells contained more EPCR⁺ cells, whereas EPCR⁺CD48⁺KSL cells clearly contained CD244⁺ cells (Figure S4). Based on our flow cytometry analysis we decided to transplant CD244⁺CD48⁺KSL, CD244⁺CD48⁺KSL, and CD244⁺CD48⁺KSL cells from the PVA culture. The transplantation experiment revealed that the highest reconstitution in PB was found within the CD244⁺CD48⁺KSL cells and significantly lower but stable long-term reconstitution was seen in CD244⁺CD48⁺KSL cells, whereas CD244⁺CD48⁺KSL failed to engraft (Figure 6C). The balance of three lineages in the PB of the long-term (16 weeks) reconstituted mice was similar between CD244⁺CD48⁺KSL and CD244⁺CD48⁺KSL cells (Figure 6D). However, analyses of BM of the transplanted mice revealed that contribution of donor cells in the HSC population was mostly observed in the CD244⁺CD48⁺HSCs-engrafted mice (Figure 6E).

These findings reveal that cells equipped with long-term reconstitution potential are limited, even when using PVA expansion medium, and that CD244 negativity is a potent marker to efficiently enrich functional HSCs after *ex vivo* expansion.

DISCUSSION

The long-term reconstitution assay has been recognized as an exclusive and conclusive method to prove the functional potential of HSCs. However, transplantation assays require a large number of recipient animals, long time periods of monitoring, and high costs. Therefore, developing methods that allow for the

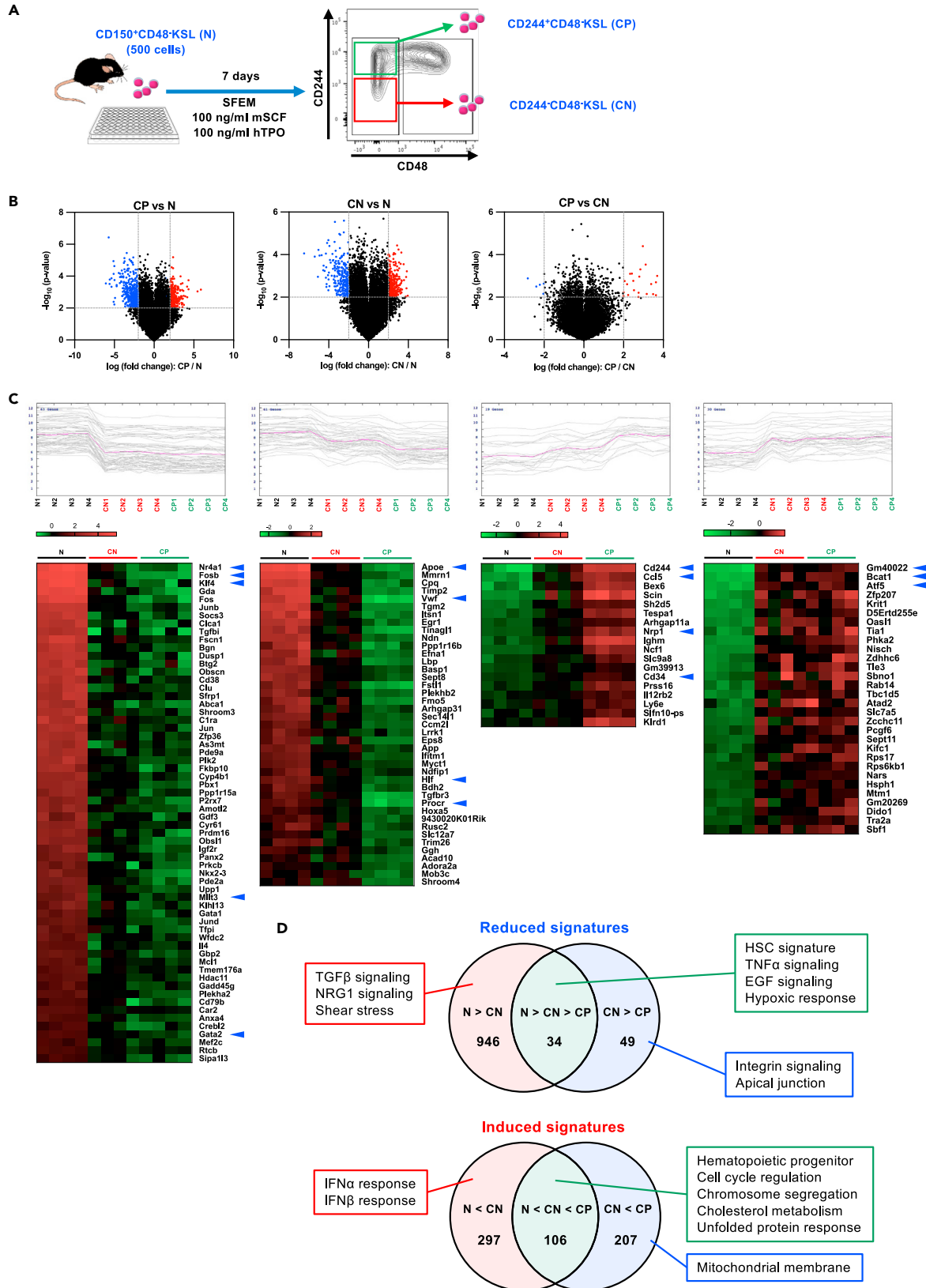


Figure 5. Gene expression profiling of CD244⁻ and CD244⁺ KSL cells

(A) Experimental design of the gene expression analysis. Five hundred CD244⁻CD48⁻KSL cells were sorted from BM of 10-week-old mice (N) and were also cultured in Stemspan SFEM medium supplemented with 100 ng/mL MSCF and 100 ng/mL hTPO for 7 days, and CD244⁻KSL (CN) and CD244⁺KSL (CP) cells were re-sorted.

(B) Volcano plot showing differentially expressed genes between CP versus N (left), CN versus N (center), and CP versus CN (right). Significant difference was defined as $p < 0.01$ and \log_2 fold change < -2 (blue) or > 2 (red).

(C) K-mean clustering of genes showing different expression patterns between the three cohorts and heatmaps of selected genes. Significant difference was defined as $p < 0.001$ and \log_2 fold change < -2 or > 2 .

(D) Overlap of hallmarks and GO terms between the three groups based on GSEA. See also [Table S2](#).

prospective evaluation of reconstitution potential of HSCs is of great benefit. The biggest challenge is to identify reliable markers that reflect reconstitution potential of HSCs under non-steady-state conditions, e.g., *in vitro* culture. This study has revealed that phenotypic murine HSCs after *in vitro* culture have quite distinct gene expression patterns, particularly the reduction of HSC genes and the induction of mast cell-related genes ([Figures 2C and 2D](#)). Although decreased expression levels of HSC-related genes may be a major part of the functional retardation, unexpected elevation of some genes is also considered a critical reason of failed reconstitution. For instance, granzyme B (*Gzmb*) has been reported to have negative impact on the long-term reconstitution potential of HSCs ([Carnevali et al., 2014](#)).

Among them, we particularly identified CD244 as a robust marker that represents the decline of reconstitution potential of murine HSCs after *in vitro* culture. CD244 expression is low on freshly isolated HSCs ([Kiel et al., 2005](#); [Oguro et al., 2013](#)); however, *in vitro* culture clearly induced CD244 expression ([Figures 3B and 3C](#)). Of note, CD244⁺CD48⁻KSL (CD244⁺HSCs) did not efficiently engraft to transplanted recipient mice, whereas CD244⁻ cells still sustained reconstitution potential ([Figure 3E](#)). The potential of CD244 negativity in combination with CD48 was further supported by experiments using a new HSC expansion system with PVA ([Wilkinson et al., 2019](#)). After culturing with the PVA system, long-term reconstitution ability was mainly found in the CD244⁻CD48⁻KSL population ([Figures 6C and 6E](#)) that comprised only 10% of the total culture. Including CD244 as a marker for *in vitro* cultured HSC is thus highly beneficial and allows for a higher-resolution comparison of gene expression profiles between freshly isolated HSCs and *in vitro* cultured HSCs.

Although functional HSCs are highly enriched in the CD244⁻CD48⁻KSL fraction after *in vitro* culture, the frequency is still lower than of fresh BM cells. This might be explained by a lack of yet-unidentified additional marker(s) to capture all functional HSC. From the gene expression analysis data ([Figures 2C and 5C](#)) we have tested some additional cell surface molecules (e.g., CD53 and *Nrp1*) but so far not found additional markers to further subdivide CD244⁻HSCs. Alternatively, such markers might not be cell surface molecules but cellular characteristics reflecting metabolic conditions.

In summary, we conclude that CD244 is an important marker to distinguish functional versus non-functional HSCs after culture. Including CD244 as a marker to evaluate *in vitro*-cultured HSCs may help to prospectively estimate reconstitution potential and therefore contribute to further improvement of *in vitro* HSC expansion systems.

Limitations of the study

This study particularly targeted murine HSC, and therefore the ability of CD244 negativity as a marker for HSC of other species, e.g., human, is unknown. In addition, whether CD244 expression is implicated in different stress conditions is unclear at this moment.

STAR★METHODS

Detailed methods are provided in the online version of this paper and include the following:

- [KEY RESOURCES TABLE](#)
- [RESOURCE AVAILABILITY](#)
 - Lead contact
 - Materials availability
 - Data and code availability
- [EXPERIMENTAL MODEL AND SUBJECT DETAILS](#)
 - Mice

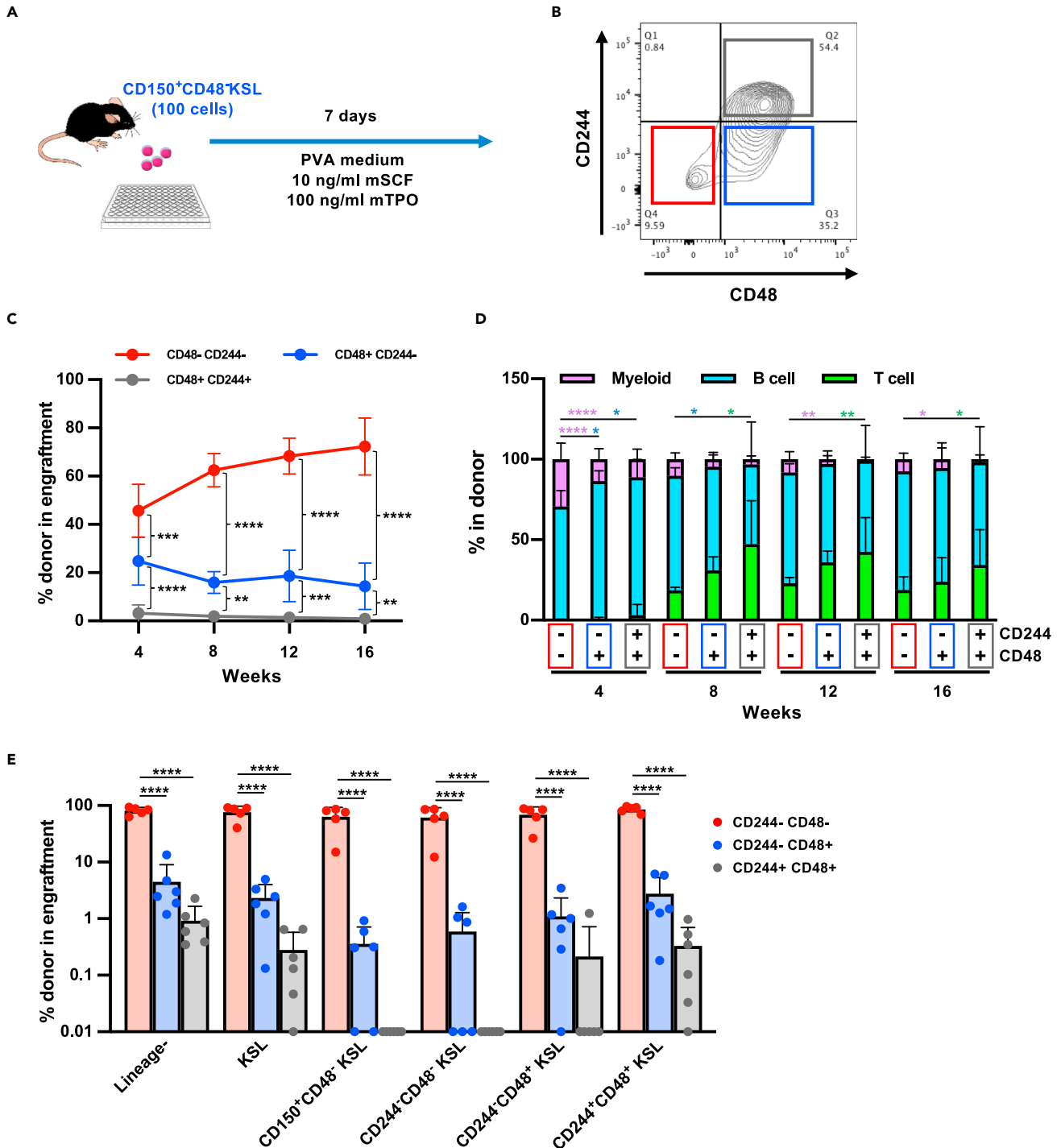


Figure 6. CD244 expression distinguishes functionally distinct subpopulations after *in vitro* culture in PVA medium

(A) Experimental design of the *in vitro* culture experiment. One hundred CD48⁺KSL cells were sorted from BM of young mice and cultured in PVA containing medium (Wilkinson et al., 2019) supplemented with 10 ng/mL mSCF and 100 ng/mL hTPO for 7 days.

(B) Expression patterns of CD244 and CD48 on the cell surface of KSL cells after *in vitro* culture in PVA medium. A representative FACS plot on KSL population is shown.

(C) Competitive reconstitution assay. After 7 days' culture, three subpopulations were sorted and 500 of CD244⁻CD48⁻KSL cells, CD244⁻CD48⁺KSL cells, or CD244⁺CD48⁺KSL cells were separately transplanted into lethally irradiated recipient mice with 2×10^5 total BM cells. Chimerism was monitored by

Figure 6. Continued

analyzing PB every month. Significance was calculated using one-way ANOVA at each time point. Mean \pm SD from two independent experiments (n = 12) are displayed. **p < 0.01, ***p < 0.001, ****p < 0.0001

(D) Lineage balance of donor-derived cells in the PB of recipient mice. Significance was calculated using one-way ANOVA at each time point. Mean \pm SD from two independent experiments (n = 12) are displayed. *p < 0.05, **p < 0.01, ****p < 0.0001. Each color represents different lineages.

(E) Analysis of BM from engrafted mice after 16 weeks. Chimerism in each cell fraction is shown. Significance was calculated using one-way ANOVA within each population. Mean \pm SD from two independent experiments (n = 5) are displayed. ****p < 0.0001.

METHOD DETAILS

- Flow cytometry
- *In vitro* culture of HSCs
- HSC culture with chemical compounds
- Cell cycle analysis
- Protein synthesis rate analysis
- Microarray analysis
- Long-term competitive repopulation assay
- Limiting dilution assay
- Quantitative RT-PCR

QUANTIFICATION AND STATISTICAL ANALYSIS**SUPPLEMENTAL INFORMATION**

Supplemental information can be found online at <https://doi.org/10.1016/j.isci.2021.103603>.

ACKNOWLEDGEMENTS

We thank Mattias Magnusson, Mark van der Garde, Terumasa Umemoto, and Satoshi Yamazaki for scientific discussions. This work was supported by JSPS Grant-in-Aid for Young Scientists (20K17370) (S.K.), Uehara Memorial Foundation (S.K.), the Swedish Child Cancer Foundation (V.S.), Åke-Wibergs foundation (V.S., K.M.), the Crafoord foundation (V.S., K.M.), the Swedish Cancer Society (V.S., V.R., K.M.), Olle Engkvist Foundation (K.S.), Grants-in-Aid for Scientific Research (JP19H05653) (A.I.), Scientific Research on Innovative Areas "Replication of Non-Genomic Codes" (JP19H05746) from MEXT, Japan (A.I.), The Swedish Research Council (K.M.), and Knut and Alice Wallenberg Foundation (K.M.). This study was also partly supported by a Grant from International Joint Usage/Research Center, the Institute of Medical Science, The University of Tokyo. K.M. was funded by StemTherapy program at Lund University. The Lund Stem Cell Center was supported by a Center of Excellence grant in life sciences from the Swedish Foundation for Strategic Research.

AUTHOR CONTRIBUTIONS

K.M. designed the project. S.K., V.S., A.I., and K.M. planned experiments. S.K., V.S., V.R., K.S., Z.Z., and K.M. performed experiments. S.K., S.L., S.S., and K.M. analyzed gene expression data. S.K., V.S., A.I., and K.M. wrote the manuscript.

DECLARATION OF INTERESTS

The authors declare no competing interests.

Received: February 12, 2021

Revised: October 28, 2021

Accepted: December 7, 2021

Published: January 21, 2022

REFERENCES

- Abraham, S.N., and St John, A.L. (2010). Mast cell-orchestrated immunity to pathogens. *Nat. Rev. Immunol.* 10, 440–452. <https://doi.org/10.1038/nri2782>.
- Agresta, L., Hoebe, K.H.N., and Janssen, E.M. (2018). The emerging role of CD244 signaling in immune cells of the tumor microenvironment. *Front. Immunol.* 9, 2809. <https://doi.org/10.3389/fimmu.2018.02809>.
- Balazs, A.B., Fabian, A.J., Esmen, C.T., and Mulligan, R.C. (2006). Endothelial protein C receptor (CD201) explicitly identifies hematopoietic stem cells in murine bone marrow. *Blood* 107, 2317–2321. <https://doi.org/10.1182/blood-2005-06-2249>.
- Carnevali, L.S., Scognamiglio, R., Cabezas-Wallscheid, N., Rahmig, S., Laurenti, E., Masuda, K., Jöckel, L., Kuck, A., Sujer, S., Polykratis, A., et al. (2014). Improved HSC reconstitution and protection from inflammatory stress and

- chemotherapy in mice lacking granzyme B. *J. Exp. Med.* 211, 769–779. <https://doi.org/10.1084/jem.20131072>.
- Calvanese, V., Nguyen, A.T., Bolan, T.J., Vavilina, A., Su, T., Lee, L.K., Wang, Y., Lay, F.D., Magnusson, M., Crooks, G.M., et al. (2019). MLLT3 governs human hematopoietic stem-cell self-renewal and engraftment. *Nature* 576, 281–286. <https://doi.org/10.1038/s41586-019-1790-2>.
- Doan, P.L., Himburg, H.A., Helms, K., Russell, J.L., Fixsen, E., Quarmyne, M., Harris, J.R., Deoliviera, D., Sullivan, J.M., Chao, N.J., et al. (2013). Epidermal growth factor regulates hematopoietic regeneration after radiation injury. *Nat. Med.* 19, 295–304. <https://doi.org/10.1038/nm.3070>.
- Dwyer, D.F., Barrett, N.A., and Austen, K.F.; Immunological Genome Project Consortium (2016). Expression profiling of constitutive mast cells reveals a unique identity within the immune system. *Nat. Immunol.* 17, 878–887. <https://doi.org/10.1038/ni.3445>.
- Elishmereni, M., Fyhrquist, N., Gangwar, R.S., Lehtimäki, S., Alenius, H., and Levi-Schaffer, F. (2014). Complex 2B4 regulation of mast cells and eosinophils in murine allergic inflammation. *J. Invest. Dermatol.* 134, 2928–2937. <https://doi.org/10.1038/jid.2014.280>.
- Fares, I., Chagraoui, J., Lehnertz, B., MacRae, T., Mayotte, N., Tomellini, E., Aubert, L., Roux, P.P., and Sauvageau, G. (2017). EPCR expression marks UM171-expanded CD34⁺ cord blood stem cells. *Blood* 129, 3344–3351. <https://doi.org/10.1182/blood-2016-11-750729>.
- Freire, P.R., and Conneely, O.M. (2018). NR4A1 and NR4A3 restrict HSC proliferation via reciprocal regulation of C/EBP α and inflammatory signaling. *Blood* 131, 1081–1093. <https://doi.org/10.1182/blood-2017-07-795757>.
- Gazit, R., Mandal, P.K., Ebina, W., Ben-Zvi, A., Nombela-Arieta, C., Silberstein, L.E., and Rossi, D.J. (2014). Fgd5 identifies hematopoietic stem cells in the murine bone marrow. *J. Exp. Med.* 211, 1315–1331. <https://doi.org/10.1084/jem.20130428>.
- Galli, S.J., and Tsai, M. (2012). IgE and mast cells in allergic disease. *Nat. Med.* 18, 693–704. <https://doi.org/10.1038/nm.2755>.
- Goodell, M.A., Brose, K., Paradis, G., Conner, A.S., and Mulligan, R.C. (1996). Isolation and functional properties of murine hematopoietic stem cells that are replicating in vivo. *J. Exp. Med.* 183, 1797–1806. <https://doi.org/10.1084/jem.183.4.1797>.
- Hu, Y., and Smyth, G.K. (2009). ELDA: extreme limiting dilution analysis for comparing depleted and enriched populations in stem cell and other assays. *J. Immunol. Methods* 347, 70–78. <https://doi.org/10.1016/j.jim.2009.06.008>.
- Kiel, M.J., Yilmaz, O.H., Iwashita, T., Yilmaz, O.H., Terhorst, C., and Morrison, S.J. (2005). SLAM family receptors distinguish hematopoietic stem and progenitor cells and reveal endothelial niches for stem cells. *Cell* 121, 1109–1121. <https://doi.org/10.1016/j.cell.2005.05.026>.
- Kobayashi, H., Morikawa, T., Okinaga, A., Hamano, F., Hashidate-Yoshida, T., Watanuki, S., Hishikawa, D., Shindou, H., Arai, F., Kabe, Y., et al. (2019). Environmental optimization enables maintenance of quiescent hematopoietic stem cells ex vivo. *Cell Rep.* 28, 145–158. <https://doi.org/10.1016/j.celrep.2019.06.008>.
- Komorowska, K., Doyle, A., Wahlestedt, M., Subramaniam, A., Debnath, S., Chen, J., Soneji, S., Van Handel, B., Mikkola, H.K.A., Miharada, K., et al. (2017). Hepatic leukemia factor maintains quiescence of hematopoietic stem cells and protects the stem cell pool during regeneration. *Cell Rep.* 21, 3514–3523. <https://doi.org/10.1016/j.celrep.2017.11.084>.
- McArdel, S.L., Terhorst, C., and Sharpea, A.H. (2016). Roles of CD48 in regulating immunity and tolerance. *Clin. Immunol.* 164, 10–20. <https://doi.org/10.1016/j.clim.2016.01.008>.
- Martelli, F., Ghinassi, B., Lorenzini, R., Vannucchi, A.M., Rana, R.A., Nishikawa, M., Partamian, S., Migliaccio, G., and Migliaccio, A.R. (2008). Thrombopoietin inhibits murine mast cell differentiation. *Stem Cells* 26, 912–919. <https://doi.org/10.1634/stemcells.2007-0777>.
- Miharada, K., Karlsson, G., Rehn, M., Rörby, E., Siva, K., Cammenga, J., and Karlsson, S. (2011). Cripto regulates hematopoietic stem cells as a hypoxic-niche-related factor through cell surface receptor GRP78. *Cell Stem Cell* 9, 330–344. <https://doi.org/10.1016/j.stem.2011.07.016>.
- Miharada, K., Sigurdsson, V., and Karlsson, S. (2014). Dppa5 improves hematopoietic stem cell activity by reducing endoplasmic reticulum stress. *Cell Rep.* 9, 330–344. <https://doi.org/10.1016/j.celrep.2014.04.056>.
- Noda, S., Horiguchi, K., Ichikawa, H., and Miyoshi, H. (2008). Repopulating activity of ex vivo-expanded murine hematopoietic stem cells resides in the CD48-c-Kit+Sca-1+ lineage marker- cell population. *Stem Cells* 26, 646–655. <https://doi.org/10.1634/stemcells.2007-0623>.
- Notta, F., Doulatov, S., Laurenti, E., Poeppl, A., Jurisica, I., and Dick, J.E. (2011). Isolation of single human hematopoietic stem cells capable of long-term multilineage engraftment. *Science* 333, 218–221. <https://doi.org/10.1126/science.1201219>.
- Oguro, H., Ding, L., and Morrison, S.J. (2013). SLAM family markers resolve functionally distinct subpopulations of hematopoietic stem cells and multipotent progenitors. *Cell Stem Cell* 13, 102–116. <https://doi.org/10.1016/j.stem.2013.05.014>.
- Osawa, M., Hanada, K., Hamada, H., and Nakauchi, H. (1996). Long-term lymphohematopoietic reconstitution by a single CD34-low/negative hematopoietic stem cell. *Science* 273, 242–245. <https://doi.org/10.1126/science.273.5272.242>.
- Özcan, U., Yilmaz, E., Özcan, L., Furuhashi, M., Vaillancourt, E., Smith, R.O., Görgün, C.Z., and Hotamisligil, G.S. (2006). Chemical chaperones reduce ER stress and restore glucose homeostasis in a mouse model of type 2 diabetes. *Science* 313, 1137–1140. <https://doi.org/10.1126/science.1128294>.
- Park, C., Lewis, A., Chen, T., and Lacorazza, D. (2019). Concise review: Regulation of self-renewal in normal and malignant hematopoietic stem cells by Krüppel-Like Factor 4. *Stem Cells Transl. Med.* 8, 568–574. <https://doi.org/10.1002/sctm.18-0249>.
- Seita, J., and Weissman, I.L. (2010). Hematopoietic stem cell: self-renewal versus differentiation. *Wiley Interdiscip Rev Syst Biol Med.* 2, 640–653. <https://doi.org/10.1002/wsbm.86>.
- Sigurdsson, V., Haga, Y., Takei, H., Mansell, E., Okamatsu-Haga, C., Suzuki, M., Radulovic, V., van der Garde, M., Koide, S., Soboleva, S., et al. (2020). Induction of blood-circulating bile acids supports recovery from myelosuppressive chemotherapy. *Blood Adv.* 4, 1833–1843. <https://doi.org/10.1182/bloodadvances.2019000133>.
- Sigurdsson, V., Takei, H., Soboleva, S., Radulovic, V., Galeev, R., Siva, K., Leeb-Lundberg, L.M., Iida, T., Nittono, H., and Miharada, K. (2016). Bile acids protect expanding hematopoietic stem cells from unfolded protein stress in fetal liver. *Cell Stem Cell* 18, 522–532. <https://doi.org/10.1016/j.stem.2016.01.002>.
- Storms, R.W., Trujillo, A.P., Springer, J.B., Shah, L., Colvin, O.M., Ludeman, S.M., and Smith, C. (1999). Isolation of primitive human hematopoietic progenitors on the basis of aldehyde dehydrogenase activity. *Proc. Natl. Acad. Sci. U S A* 96, 9118–9123. <https://doi.org/10.1073/pnas.96.16.9118>.
- Subramanian, A., Tamayo, P., Mootha, V.K., Mukherjee, S., Ebert, B.L., Gillette, M.A., Paulovich, A., Pomeroy, S.L., Golub, T.R., Lander, E.S., et al. (2005). Gene set enrichment analysis: A knowledge-based approach for interpreting genome-wide expression profiles. *Proc. Natl. Acad. Sci. U S A* 102, 15545–15550. <https://doi.org/10.1073/pnas.0506580102>.
- Suda, T., Takubo, K., and Semenza, G.L. (2011). Metabolic regulation of hematopoietic stem cells in the hypoxic niche. *Cell Stem Cell* 9, 298–310. <https://doi.org/10.1016/j.stem.2011.09.010>.
- Sudo, K., Ema, H., Morita, Y., and Nakauchi, H. (2000). Age-associated characteristics of murine hematopoietic stem cells. *J. Exp. Med.* 192, 1273–1280. <https://doi.org/10.1084/jem.192.9.1273>.
- Umamoto, T., Hashimoto, M., Matsumura, T., Nakamura-Ishizu, A., and Suda, T. (2018). Ca²⁺-mitochondria axis drives cell division in hematopoietic stem cells. *J. Exp. Med.* 215, 2097–2113. <https://doi.org/10.1084/jem.20180421>.
- van Galen, P., Kreso, A., Mbong, N., Kent, D.G., Fitzmaurice, T., Chambers, J.E., Xie, S., Laurenti, E., Hermans, K., Eppert, K., et al. (2014). The unfolded protein response governs integrity of the haematopoietic stem-cell pool during stress.

Nature 510, 268–272. <https://doi.org/10.1038/nature13228>.

Waggoner, S.N., and Kumar, K. (2012). Evolving role of 2B4/CD244 in T and NK cell responses during virus infection. *Front. Immunol.* 3, 377. <https://doi.org/10.3389/fimmu.2012.00377>.

Walter, P., and Ron, D. (2011). The unfolded protein response: from stress pathway to homeostatic regulation. *Science* 334, 1081–1086. <https://doi.org/10.1126/science.1209038>.

Wilkinson, A.C., Ishida, R., Kikuchi, M., Sudo, K., Morita, M., Crisostomo, R.V., Yamamoto, R., Loh, K.M., Nakamura, Y., Watanabe, M., et al. (2019). Long-term ex vivo haematopoietic-stem-cell expansion allows nonconditioned transplantation. *Nature* 571, 117–121. <https://doi.org/10.1038/s41586-019-1244-x>.

Yamashita, M., and Passegué, E. (2019). TNF- α coordinates hematopoietic stem cell survival and myeloid regeneration. *Cell Stem Cell* 25, 357–372. <https://doi.org/10.1016/j.stem.2019.05.019>.

Yamazaki, S., Iwama, A., Takayanagi, S., Eto, K., Ema, H., and Nakauchi, H. (2009). TGF-beta as a candidate bone marrow niche signal to induce hematopoietic stem cell hibernation. *Blood* 113, 1250–1256. <https://doi.org/10.1182/blood-2008-04-146480>.

Zhang, C.C., and Lodish, H.F. (2005). Murine hematopoietic stem cells change their surface phenotype during ex vivo expansion. *Blood* 105, 4314–4320. <https://doi.org/10.1182/blood-2004-11-4418>.

STAR★METHODS

KEY RESOURCES TABLE

REAGENT or RESOURCE	SOURCE	IDENTIFIER
Antibodies		
Rat anti-mouse B220 (RA3-6B2), APC	BioLegend	Cat# 103212; RRID: AB_312997
Rat anti-mouse B220 (RA3-6B2), PE/Cy5	BioLegend	Cat# 103210; RRID: AB_312995
Armenian Hamster anti-mouse CD3 ϵ (145-2C11), APC	BioLegend	Cat# 100312; RRID: AB_312677
Armenian Hamster anti-mouse CD3 ϵ (145-2C11), Biotin	BioLegend	Cat# 100304; RRID: AB_312669
Armenian Hamster anti-mouse CD3 ϵ (145-2C11), PE/Cy5	BioLegend	Cat# 100310; RRID: AB_312675
Rat anti-mouse CD4 (L3T4), APC/Cy7	BioLegend	Cat# 100526; RRID: AB_312727
Rat anti-mouse CD4 (GK1.5), Biotin	BioLegend	Cat# 100404; RRID: AB_312689
Rat anti-mouse CD4 (H129.19), FITC	BioLegend	Cat# 130308; RRID: AB_1279237
Rat anti-mouse CD8a (53-6.7), APC/Cy7	BioLegend	Cat# 100714; RRID: AB_312747
Rat anti-mouse CD8a (53-6.7), PE	BioLegend	Cat# 100708; RRID: AB_312747
Rat anti-mouse CD11b (M1/70), Biotin	BioLegend	Cat# 101204; RRID: AB_312787
Rat anti-mouse CD11b (M1/70), PE	BioLegend	Cat# 101208; RRID: AB_312791
Rat anti-mouse CD11b (M1/70), PE/Cy5	BioLegend	Cat# 101210; RRID: AB_312793
Mouse anti-mouse CD45.1 (A20), Brilliant Violet 510™	BioLegend	Cat# 110741; RRID: AB_2563378
Rat anti-mouse CD45.1 (A20), PE/Cy7	BioLegend	Cat# 110730; RRID: AB_1134168
Rat anti-mouse CD45.1 (A20), PerCP	BioLegend	Cat# 110726; RRID: AB_893345
Mouse anti-mouse CD45.2 (104), APC	BioLegend	Cat# 109814; RRID: AB_389211
Mouse anti-mouse CD45.2 (104), FITC	BioLegend	Cat# 109806; RRID: AB_313443
Mouse anti-mouse CD45.2 (104), Brilliant Violet 421™	BioLegend	Cat# 109832; RRID: AB_2565511
Mouse anti-mouse CD45.2 (104), Brilliant Violet 785™	BioLegend	Cat# 109839; RRID: AB_2562604
Mouse anti-mouse CD45.2 (104), PE	BioLegend	Cat# 109808; RRID: AB_313445
Rat anti-mouse CD48 (HM48-1), APC	BioLegend	Cat# 103412; RRID: AB_571997
Rat anti-mouse CD48 (HM48-1), FITC	BioLegend	Cat# 103404; RRID: AB_313019
Rat anti-mouse CD150 (TC15-12F12.2), PE/Cy7	BioLegend	Cat# 115914; RRID: AB_439797
Rat anti-mouse CD244.2 (m2B4), PE	BioLegend	Cat# 133508; RRID: AB_2072855
Rat anti-mouse c-kit (2B8), APC	BioLegend	Cat# 105812; RRID: AB_313221
Rat anti-mouse c-kit (2B8), APC/Cy7	BioLegend	Cat# 105826; RRID: AB_1626278
Armenian Hamster anti-mouse Fc ϵ R1 α (MAR-1), FITC	BioLegend	Cat# 134306; RRID: AB_1626108
Rat anti-mouse Ly-6G/Ly-6C (Gr-1) (RB6-8C5), PE	BioLegend	Cat# 108408; RRID: AB_313373
Rat anti-mouse Ly-6G/Ly-6C (Gr-1) (RB6-8C5), PE/Cy5	BioLegend	Cat# 108410; RRID: AB_313375
Rat anti-mouse Ly-6A/E (Sca-1) (D7), FITC	BioLegend	Cat# 108106; RRID: AB_313343
Rat anti-mouse Ly-6A/E (Sca-1) (D7), Brilliant Violet 421™	BioLegend	Cat# 108127; RRID: AB_2563064
Rat anti-mouse Ter119 (TER119), Biotin	BioLegend	Cat# 116204; RRID: AB_313705
Rat anti-mouse Ter119 (TER119), PE/Cy5	BioLegend	Cat# 116210; RRID: AB_313711
Streptavidin-APC	BioLegend	Cat# 405207
Streptavidin-Brilliant Violet 605™	BD	Cat# 563260
Rat anti-mouse CD34 (RAM34), FITC	eBioscience	Cat# 11-0341-85; RRID: AB_465021
Rat anti-mouse CD201 (eBio1560), APC	eBioscience	Cat# 17-2012-82; RRID: AB_10717805
Rat anti-mouse c-kit (2B8), APC-eFluor 780	Thermo Fisher Scientific	Cat# 47-1171-82; RRID: AB_1272177
Rat anti-mouse CD8a (53-6.7), Biotin	TONBO	Cat# 20-0081-U100

(Continued on next page)

Continued

REAGENT or RESOURCE	SOURCE	IDENTIFIER
Chemicals, peptides, and recombinant proteins		
7-Amino-Actinomycin-D (7AAD)	Sigma-aldrich	Cat# A9400-1MG
CD117 MicroBeads, mouse	Miltenyi Biotec	Cat# 130-091-224
Recombinant Murine stem cell factor (mSCF)	PEPROTECH	Cat# 250-03-10 µg
Recombinant Mouse thrombopoietin (mTPO)	PEPROTECH	Cat# AF-315-14-10 µg
Recombinant Human thrombopoietin (hTPO)	PEPROTECH	Cat# 300-18-10µg
2-Mercaptoethanol	Sigma-aldrich	Cat# M6250-100ML
Ham's F-12 Nutrient Mix	Gibco	Cat# 11765054
StemSpan™ SFEM	Stem Cell Technologies	Cat# 09650
HEPES	Thermo Fisher Scientific	Cat# 15630080
Penicillin–Streptomycin–Glutamine	Thermo Fisher Scientific	Cat# 10378016
Insulin–Transferrin–Selenium–Ethanolamine (ITS-X)	Thermo Fisher Scientific	Cat# 51500056
Polyvinyl alcohol (87–90%-hydrolyzed)	Sigma-Aldrich	Cat# P8136-250G
Taurochenodeoxycholic acid	Sigma-Aldrich	Cat# T6260
Taurocholic acid	Sigma-Aldrich	Cat# T9034
Tauro- α -muricholic acid	Toronto Research Chemicals	Cat# T009130
Tauro- β -muricholic acid	Santa Cruz	Cat# sc-361829
Tauroursodeoxycholic acid	Sigma-Aldrich	Cat# T0266
Critical commercial assays		
RNeasy Micro Kit	QIAGEN	Cat# 74004
Ki-67 staining Kit	BD	Cat# 556026
Click-IT™ L-Homopropargylglycine (HPG)	Thermo Fisher Scientific	Cat# C10186
Click-iT™ Plus Alexa Fluor™ 488 Picolyl Azide Toolkit	Thermo Fisher Scientific	Cat# C10641
BD Cytofix/Cytoperm™ Fixation/Permeabilization Solution Kit	Thermo Fisher Scientific	Cat# BDB554714
Deposited data		
Microarray analysis	NCBI Gene Expression Omnibus (GEO) database	Accession number: GSE162408
Experimental models: Organisms/strains		
Mouse: C57BL/6 (CD45.2)	Taconic	N/A
Mouse: B6.SJL (CD45.1)	In-house breeding	N/A
Oligonucleotides		
Quantitative real-time PCR probe for <i>Cpa3</i>	Thermo Fisher Scientific	Mm00483940_m1
Quantitative real-time PCR probe for <i>Fcer1a</i>	Thermo Fisher Scientific	Mm00438867_m1
Quantitative real-time PCR probe for <i>Fgd5</i>	Thermo Fisher Scientific	Mm01189735_g1
Quantitative real-time PCR probe for <i>Fhl1</i>	Thermo Fisher Scientific	Mm04204611_g1
Quantitative real-time PCR probe for <i>Gzmb</i>	Thermo Fisher Scientific	Mm00442834_m1
Quantitative real-time PCR probe for <i>Hlf</i>	Thermo Fisher Scientific	Mm00723157_m1
Quantitative real-time PCR probe for <i>Hprt</i>	Thermo Fisher Scientific	Mm03024075_m1
Quantitative real-time PCR probe for <i>Ldhd</i>	Thermo Fisher Scientific	Mm01267402_m1
Quantitative real-time PCR probe for <i>Mpl</i>	Thermo Fisher Scientific	Mm00440310_m1
Software and algorithms		
Gene Expression Commons	RIKEN	https://gexc.riken.jp/
FlowJo	Tree Star	N/A
ELDA	WEHI	https://bioinf.wehi.edu.au/software/elda/
Prism	Graphpad	N/A

RESOURCE AVAILABILITY

Lead contact

Further information and requests for resources and reagents should be directed to and will be fulfilled by the lead contact, Kenichi Miharada (kenmiharada@kumamoto-u.ac.jp).

Materials availability

This study did not generate new unique reagents.

Data and code availability

- Microarray data have been deposited at GEO and are publicly available as of the date of publication. Accession number is listed in the [key resources table](#).
- This paper does not report original code.
- Any additional information required to reanalyze the data reported in this paper is available from the lead contact upon request.

EXPERIMENTAL MODEL AND SUBJECT DETAILS

Mice

B6.SJL (Ly-5.1) male mice (8-10 weeks old) were obtained from The Jackson Laboratory. Young (10 weeks old) and aged (18 months old) C57BL/6J (Ly-5.2) male mice were obtained from Janvier Labs. All animals were maintained in individually ventilated racks and given autoclaved food and water ad libitum. All experiments were approved by the Lund University Animal Ethical Committee, Swedish Board of Agriculture and Animal Research Facility of The University of Tokyo guidelines.

METHOD DETAILS

Flow cytometry

Adult BM cells were isolated by crushing tibias, femurs and iliac bones of 8 to 10 weeks old mice with a mortar and pestle in PBS. c-Kit positive (c-Kit⁺) cells were enriched using magnetic separation system (MACS) with anti-c-Kit magnetic beads (Miltenyi Biotec). The enriched cells were stained with a combination of antibodies (please see [STAR Methods](#) for detail) All antibodies were used at a concentration of 1:250. Anti-CD3, -B220, -CD11b, -Gr-I and Ter119 antibodies were used as lineage antibody mix. Dead cells were excluded using 7-Amino-Actinomycin-D (7AAD) staining. Cells were sorted on FACS Aria III or analyzed on FACS LSRII or LSR Fortessa (BD). Collected data were analyzed on the FlowJo software (Tree Star).

In vitro culture of HSCs

In conventional setting, CD150⁺CD48⁻KSL cells were sorted from 10 weeks old mice and cultured in StemSpan™ SFEM medium (STEMCELL Technologies) supplemented with 100 ng/mL of mouse stem cell factor (mSCF) and 100 ng/mL of human thrombopoietin (hTPO) for 7 or 14 days. Alternatively, cells were cultured in PVA containing medium ([Wilkinson et al., 2019](#)) for 7 days. Briefly, 10 mM HEPES, 1 × Penicillin–streptomycin–glutamine, 1 × Insulin–transferrin–selenium–ethanolamine (all Thermo Fischer) and 1 mg/mL polyvinyl alcohol (87–90%-hydrolyzed, Sigma-Aldrich) were added to F12 medium, and conditioned medium was supplemented with 10 ng/mL of mSCF and 100 ng/mL of mouse thrombopoietin (mTPO).

HSC culture with chemical compounds

Different types of primary bile acids (taurooursodeoxycholic acid: TUDCA, taurochenodeoxycholic acid: TCDCA, taurocholic acid: TCA, tauro- α -muricholic acid: T α MCA, tauro- β -muricholic acid: T β MCA) were dissolved in water or ethanol, and separately added to the cell culture with the concentration of 100 μ M. Tunicamycin was dissolved in water and added to the culture with the concentration of 0.5 μ g/mL.

Cell cycle analysis

Freshly isolated total BM cells or *in vitro* cultured cells were stained with HSC markers including CD244, and then fixed and permeabilized using BD Cytofix/Cytoperm Fixation and Permeabilization Kit (BD). Fixed

cells were then stained with anti-Ki67 antibody and DAPI. Cell cycle status was determined based on the Ki-67 expression and DNA replication on FACS Fortessa.

Protein synthesis rate analysis

Protein synthesis rate was measured using L-homopropargylglycine (L-HPG) incorporation into newly synthesized proteins. HSCs were culture in standard conditions as described above. 50 μ M L-HPG in fresh medium was added to cells on day 7 and incubated for 30 min. After surface staining for HSC markers, cells were fixed and permeabilized using BD Cytotfix/cytoperm kit. L-HPG was detected with an Alexa Fluor 488 azide using Click-iT plus. MFI measurements were done in different populations of cultured cells using FACS Aria III.

Microarray analysis

To compare gene expression profiles of freshly isolated HSCs and cultured HSCs, CD48⁻KSL cells were sorted from BM of 10 weeks old or 18 months old C57BL/6 SJL mice. A part of young HSCs were then cultured in the conventional condition, and 14-days later CD48⁻KSL fraction was re-sorted. Total RNA was isolated from the sorted cells using RNeasy[®] Micro Kit (Qiagen) according to the manufacturer's protocol. After the quality/quantity determination of the extracted RNA, cDNA was synthesized and amplified using Ovation[®] Pico WTA System V2 (NuGEN).

In order to compare gene expression profiles of CD244⁻ and CD244⁺HSCs, CD244⁻CD48⁻KSL cells were sorted from BM of 10 weeks old mice, and a part of cells were cultured in the conventional condition, and 7 days later CD244⁻CD48⁻KSL and CD244⁺CD48⁻KSL fractions were re-sorted. Total RNA was isolated as mentioned above. After the quality/quantity determination, extracted RNA was amplified and converted to cDNA using GeneChip[®] 3' IVT Pico Reagent Kit (Affymetrix).

Fragmented and labeled double-strand cDNA were hybridized to Affymetrix Mouse Genome 430 PM Array Plates using an Affymetrix GeneTitan[®] system controlled by the Affymetrix GeneChip[®] Command Console[®] software v4.2 or v4.3.3. The fluorescent signals were measured with an Affymetrix GeneTitan[®] system controlled by the Affymetrix GeneChip[®] Command Console[®] software v4.2 or v4.3.3. Gene level summarized probe set signals in log₂ scale were calculated from Affymetrix CEL files by using the RMA algorithm as implemented in the Affymetrix GeneChip[®] Expression Console[®] v1.4 Software. Sample processing was performed at a Genomics Core Facility, "KFB - Center of Excellence for Fluorescent Bioanalytics" (Regensburg, Germany; www.kfb-regensburg.de). Differential genes were called using the Limma R package using a p value cut off of 0.01 or 0.05. Gene clustering was performed using k-means/medians clustering on MeV v4.8. Overlap of differentially expressed genes between multiple cohorts were defined using an online tool Venny v2.1 (<https://bioinfogp.cnb.csic.es/tools/venny/>). The microarray data are available at the GEO database under the accession number GSE162408.

Long-term competitive repopulation assay

Competitive repopulation assay was performed using the CD45 congenic mouse system. Ten to fifteen hundred (1,000-1,500) freshly isolated various HSC populations (donor) were mixed with 2×10^5 total BM cells (competitor), and then transplanted into mice irradiated with 900 cGy (recipient). Every 4 weeks after transplantation, PB from tail vein of recipient mice was collected and stained with anti-CD45.1, -CD45.2, -CD3, -Gr-1, -CD11b, and -B220 antibodies after red blood cell lysis using NH₄Cl. After long-term (16 weeks) monitoring, BM of the engrafted primary recipient mice was analyzed. Donor contribution (chimerism) was determined as a formula of % donor/(% donor + % competitor) \times 100.

Limiting dilution assay

Different number (200, 40, 10) of CD244⁻CD48⁻KSL cells re-isolated from 7 days cultured HSC were transplanted with 2×10^5 total BM cells as competitor cells into lethally irradiated recipient mice. Every 4 weeks after transplantation, PB was analyzed. Chimerism exceeding 1% in PB at 16-weeks was judged as a successful engraftment.

Quantitative RT-PCR

CD244⁻ or CD244⁺ CD48⁻KSL cells were directly sorted into lysis buffer, and total RNA was isolated using RNeasy Micro Kit. CT values were averaged, and relative expression compared to HPRT was calculated using $2^{-\Delta\text{CT}}$ formula. For the information about used probes, please see [STAR methods](#).

QUANTIFICATION AND STATISTICAL ANALYSIS

Statistical significance was determined using the Bon-ferroni method for comparison of multiple groups or the two-tailed Student's t-test for comparison of two groups. Details of used method are described in Figure Legends. All statistical analyses were performed on Prism (GraphPad).

The frequency of HSCs in the limiting dilution assay was calculated using ELDA ([Hu and Smyth, 2009](#)).